Stem Cells Translational Medicine, 2025, **14**, szae090
https://doi.org/10.1093/stcltm/szae090
Advance access publication 11 February 2025
Original Research

Assessment of immune modulation strategies to enhance survival and integration of human neural progenitor cells in rodent models of spinal cord injury

Zijian Lou[1,2], Alex Post[1,2], Narihito Nagoshi[1,3], James Hong[1], Nader Hejrati[1], Jonathon Chon Teng Chio[1,4], Mohamad Khazaei[*,1], and Michael G. Fehlings[*,1,2,4,]

[1]Division of Genetics and Development, Krembil Brain Institute, University Health Network, Toronto, ON, Canada M5T 0S8,
[2]Institute of Medical Sciences, University of Toronto, Toronto, ON, Canada M5S 1A8,
[3]Department of Orthopaedics, Keio University, Minatro City, Tokyo, JPXV+H5 Minato City, Japan,
[4]Department of Surgery, University of Toronto, Toronto, ON, Canada M5T 1P5

[*]Corresponding authors. Michael G. Fehlings, MD, PhD. E-mail: michael.fehlings@uhn.ca; ; Mohamad Khazaei, PhD, Suite 4W-449, Toronto, ON, Canada M5T 2S8. E-mail: mkhazaei@uhnres.utoronto.ca.

Abstract

Regenerative therapies are currently lacking for spinal cord injury (SCI). Neural progenitor cells (NPCs) have emerged as a promising therapeutic approach. To facilitate translation of NPCs into the clinic, studying human NPCs in rodent models is required. The preclinical study of human NPCs in rodent models of SCI necessitates an optimal selection of immunomodulatory strategies, requiring a balance between modulating the immune system and preserving its functionality.

Key words: spinal cord injury; neural progenitor cells; transplantation; gene expression; immunosuppression.

Graphical Abstract

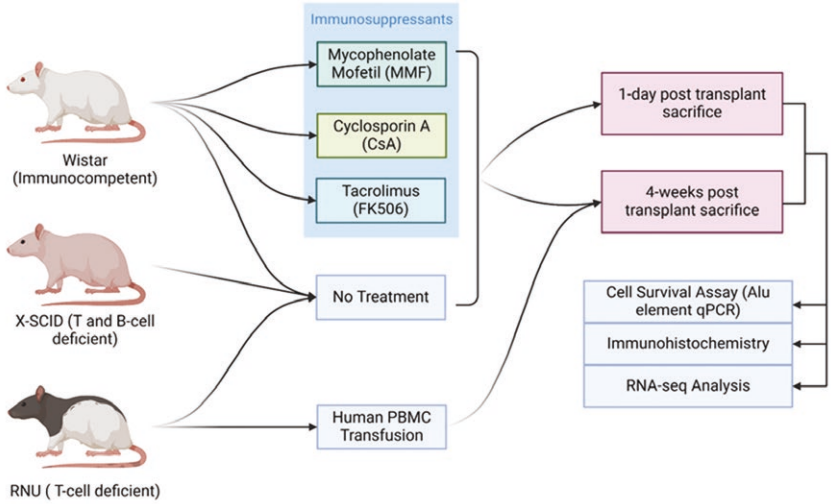

This study explores how various immunomodulatory strategies impact the survival, differentiation, and transcriptomic profiles of human iPSC-derived neural progenitor cells (NPCs) in spinal cord injury (SCI) xenograft models. Using immunocompetent, immunosuppressed, and immunodeficient rats, we identify critical differences in NPC integration and gene expression. Balanced immune modulation is key for enhancing NPC survival and functional integration in SCI therapies.

Received: 10 February 2024; Accepted: 30 October 2024.

Significance Statement

Our study demonstrates the advantage of using genetically immunodeficient rodents over traditional pharmacological methods in cell therapy research for spinal cord injury (SCI). This approach preserves the integrity and functionality of neural progenitor cells, which are essential for successful neurogenesis and neuron development. This advancement not only enhances the reliability and effectiveness of future SCI treatments but also sets a new standard in preclinical testing of regenerative medicine. Our findings have far-reaching implications, offering a promising path towards more effective and efficient therapies for SCI and potentially other neurological disorders.

Introduction

Spinal cord injury (SCI) remains a devastating condition with limited therapeutic options, affecting millions worldwide and presenting significant challenges in treatment and rehabilitation.[1] Despite advances in acute care and rehabilitation strategies, effective treatments to promote substantial functional recovery remain elusive. In recent years, cell-based therapies, particularly those utilizing human-induced pluripotent stem cell-derived neural progenitor cells (hiPSC-NPCs), have emerged as a promising avenue for SCI treatment.[2-4]

The complexity of SCI arises not just from the initial mechanical damage but also from the subsequent cascade of biological responses, including a robust immune reaction.[5-8] While this immune activation is essential to protect against potential infections, it also intensifies the severity of the injury, making the post-SCI environment more challenging for therapeutic interventions.[9,10] The disruption of the blood-spinal cord barrier (BSCB) after SCI leads to the influx of immune cells, particularly T and B lymphocytes, and the activation of resident microglia and astrocytes, which significantly impact the spinal cord's microenvironment. This influences both the progression of the injury and the potential efficacy of therapeutic interventions.[8]

Before these potential therapies can be translated to human clinical trials, rigorous pre-clinical testing in animal models is essential. However, the use of human cells in animal models creates a unique challenge: xenograft rejection. The host immune response in these xenograft models can lead to the destruction of transplanted human cells, severely limiting their survival and therapeutic potential.[11] This immune-mediated cell loss not only reduces the survival of transplanted cells but also impacts their ability to integrate functionally within the host tissue and contribute to repair processes.

Crucially, the interaction between the host immune system and transplanted human NPCs is not unidirectional but reciprocal. The presence or absence of specific immune cell populations, particularly T and B cells, in the host environment can profoundly influence the behavior of transplanted human NPCs. This cell-cell interaction, or lack thereof, has significant implications for the cellular behavior of the transplanted cells, manifesting in alterations to their gene expression profiles.[12] These changes in gene expression, particularly in transcription factors, can subsequently affect the differentiation trajectory of the NPCs.[13] The resulting alterations in differentiation patterns ultimately influence the functional integration and therapeutic efficacy of the neural cells derived from the transplanted NPCs.[14]

The importance of effective immunomodulation in xenograft models of cell transplantation for SCI cannot be overstated. Immunosuppressive strategies are crucial not only for enhancing the survival of transplanted human cells in animal models but also for creating an environment conducive to their functional integration and therapeutic efficacy.[15] However, current approaches to immunosuppression in pre-clinical xenograft studies present significant limitations and variability. Pharmacological immunosuppressants, such as cyclosporine A (CsA), tacrolimus (FK506), and mycophenolate mofetil (MMF), are commonly used in xenograft studies. While these agents can enhance graft survival, they also significantly impact the spinal cord's microenvironment, influencing the transcriptome as well as molecular and cellular behavior of transplanted human NPCs. This complex interplay between the host immune system and transplanted NPCs is further complicated by the effects of host immune cells on the gene expression of transplanted cells, which in turn affects their cellular behavior and differentiation potential.[16,17] Moreover, these immunosuppressants may not fully replicate the immune environment that would be present in human patients receiving autologous or allogeneic cell transplants.[18-20]

An alternative approach in pre-clinical xenograft studies is the use of genetically immunodeficient animal models, such as athymic Rowett nude rats (RNU) or severe combined immunodeficiency (SCID) rats. These models lack functional T cells or both T and B cells, respectively, potentially providing a more permissive environment for xenograft survival.[21-23] However, the absence of these immune components may also alter the inflammatory and regenerative processes following SCI, potentially limiting the translational relevance of findings from these models.[24] Furthermore, the lack of T and/or B cells in these models may significantly alter the reciprocal interactions between the host environment and transplanted NPCs, potentially leading to different gene expression profiles, differentiation patterns, and functional outcomes compared to immunocompetent models.[25]

The complexity of modeling human cell transplantation in animal SCI models, coupled with the need for appropriate immunomodulation, highlights a critical gap in our current understanding of how different immunomodulatory strategies in pre-clinical xenograft models impact the survival, integration, and functionality of transplanted human NPCs in the context of SCI. Optimizing pre-clinical protocols by comparing different immunomodulatory approaches in xenograft models can help identify strategies that maximize human NPC survival and integration while minimizing adverse effects on the host animal. Understanding the impact of different immunomodulatory environments on human cell behavior in animal models is crucial for designing more predictive pre-clinical studies and reducing the translational gap to human clinical trials. Additionally, insights gained from comparing genetic immunodeficiency models with pharmacological immunosuppression in xenografts can guide the development of more effective immunomodulation approaches for future clinical applications.

To address these critical issues, this study aims to explore how genetic immunodeficiency models compare to

pharmacological immunosuppression in modulating the survival, integration, and transcriptomic profiles of transplanted human iPSC-derived neural progenitor cells in rodent models of SCI.

To answer this question, we employ a multifaceted approach using three distinct rat models in a xenograft paradigm: wild-type Wistar rats treated with various immunosuppressants (CsA, FK506, MMF), T-cell deficient Rowett Nude (RNU) rats, and severely immunodeficient X-linked severe combined immunodeficiency (X-SCID) rats. By transplanting hiPSC-derived NPCs into these different immune environments and conducting comprehensive analyses, we aim to quantitatively assess human NPC survival and retention across different immunomodulatory contexts in rodent SCI models. We will evaluate the impact of various immunosuppressive strategies on host animal health and human NPC functionality in the xenograft setting, characterize the transcriptomic profiles of transplanted human NPCs in different rodent immune environments to understand how immunomodulation affects their gene expression, differentiation trajectories, as well as cellular behavior, and identify optimal immunomodulatory conditions for xenograft studies that balance human NPC survival and functionality with host well-being.

This comparative approach in pre-clinical xenograft models allows us to dissect the complex interplay between the host immune system and transplanted human NPCs, providing crucial insights that can inform the design of future pre-clinical studies and, ultimately, clinical trials. By systematically addressing these objectives, our study seeks to bridge critical gaps in the current understanding of immunomodulation in xenograft models of cell transplantation therapies for SCI, paving the way for more effective and translatable cell-based therapies for patients with spinal cord injuries.

Materials and methods

Injury and cell transplantation

Adult female Wistar rats, Rowett nude rats (RNU; NIH-Foxn1 rnu) (Charles River), and X-SCID rats (*Prkdc-/-*) (original breeder pair obtained from Horizon Labs), were anaesthetized with isoflurane (5% induction; 2—2.5% maintenance) delivered in a 1:1 ratio of O_2:N_2O and underwent a C6-7 laminectomy, as described previously.[26] Female rats were chosen due to their smaller size and easier handling when compared to their male counterparts. Briefly, a modified aneurysm clip calibrated to exert 23 grams of force was applied to the rat spinal cord between the C6 and C7 level for 1 minute, simulating a contusion-compression injury. Muscles and skin were closed with sutures and animals were treated post-operatively with buprenorphine twice a day for 3 days, meloxicam once daily for 5 days, and 10ml of saline daily for 7 days. Nine days post-injury, the rats were anesthetized to be transplanted with human-iPSC-derived NPCs, prepared as described below. The spinal cord was re-exposed, and the dura mater was dissected to allow for ease of injection. The NPCs for transplantation were differentiated from iPSCs using the dual-SMAD inhibition protocol, which involves the application of SB431542 and LDN193189 to inhibit TGF-β and BMP signaling, respectively, guiding the cells towards a neural lineage, as described previously[27], and transfected with GFP-NLS under the EF1α promoter in a piggyBac transposon vector. The hiPSC-NPCs were injected 1 mm deep into 4 sites, each injection 1 mm caudal or rostral to the epicenter of the lesion and 1 mm on either side of the midline. Each site was injected with 2 µL at 50,000 cells/µL per site at a speed of 1 µL/minute. All animal care and experimental procedures were conducted in strict accordance with the ethical guidelines and regulations set forth by the Animal Care Facility of the University Health Network (UHN), Toronto, Canada. The study protocol was reviewed and approved by the UHN Institutional Animal Care and Use Committee.

Immunosuppressant treatment

Tacrolimus (FK506) was subcutaneously administered to the rats at 1 mg/kg of animal body weight in the morning and 2 mg/kg of animal body weight in the afternoon for a total of 3 mg/kg of animal body weight per day from the cell transplantation date until the animals were sacrificed. The FK506 formulation was supplied by Chiron Pharmacy (Guelph, Ontario). Cyclosporin A (Sandimmune; Novartis, East Hanover, NJ) was subcutaneously administered to the rats daily at 10 mg/kg of animal body weight from the date of transplantation to the animal end point. Mycophenolate mofetil (CellCept, Roche, DIN 02240347) was subcutaneously administered to the rats at 30 mg/kg of animal body weight daily, from 3 days before cell transplantation until the animals were sacrificed.

Immunohistochemistry/immunofluorescent staining

Rats were perfused with 60 mL of ice-cold 1× phosphate-buffered saline (PBS) and 180 mL of paraformaldehyde (Sigma-Aldrich) (4%, w/v, in 1× PBS, pH 7.4). Two centimeters of the spinal cord (centered at the injury epicenter) was dissected and post-fixed for 5 hours with 10% sucrose (Bioshop, Burlington, ON, Canada) in a 4% PFA-PBS solution. The spinal cord was subsequently cryoprotected in 30% sucrose PBS solution. The spinal cord tissue was embedded in M1 media (Thermo Fisher Scientific) and stored at −80 °C. Spinal cords were cryosectioned at 30 µm thickness. Frozen tissue sections were stained with various antibodies diluted with blocking solution made of 1× PBS containing 5% (w/v) milk (Bioshop), 1% (w/v) bovine serum albumin (Sigma-Aldrich), and 0.03% Triton X-100 (Thermo Scientific). Tissue sections were blocked for 1 hour in room temperature with blocking solution. Subsequently, tissues were stained overnight at 4 °C using 1:100 rabbit anti-rat Iba-1 (Wako, Richmond, VA, USA, 019-19741), 1:500 FITC adsorbed rabbit anti-rat PMN (Cedarlane, Burlington, ON, Canada, CLFAD51140), 1:500 anti-human nuclear antigen nucleic marker (Abcam, ab191181), 1:500 CD19 polyclonal Antibody (Thermo Fisher Scientific, BS-0079R), or 1:500 CD3 monoclonal antibody (Biolegend, Cat 201401). The next day, tissue was washed three times (each for five minutes) with 1× PBS. For fluorescent imaging, secondary antibody (Thermo Fisher Scientific, MA, USA, goat anti-rabbit AlexaFluor 568; A-11011) was then diluted in the blocking buffer (1:500) and the tissue was incubated for 2 hours. Secondary antibody alone (no primary antibody) served as the negative control. Washing steps after antibody application were accomplished with 1× PBS washes three times each for 10 minutes, with the last wash also containing 1:1000 DAPI (4´,6-diamidino-2-phenylindole) to counterstain for nuclei. Slides were mounted onto coverslips using Mowiol (Sigma Aldrich). Images at 10× and 40× magnification were photographed with epifluorescent microscopy (Nikon Eclipse E800). For DAB imaging, tissue sections were

washed after primary antibodies were incubated overnight with PBS 3 times for 5 minutes, and stained with DAB stain (Abcam, ab64238), freshly prepared using the manufacturer instructions, for 20 minutes. The slides were washed in PBS 2 times for 5 minutes in glass chambers and then washed again with ddH_2O 3 times. Slides then underwent dehydration using 5-minute washes of an increasing gradient of 70%, 80%, 95%, and then twice 100% ethanol in ddH_2O. Tissue sections were then washed twice in Xylene and dried at room temperature for approximately 10 minutes until a visible color change was observed. Coverslips were mounted using the xylene based mounting medium (VWR, CA27900-278) and imaged using light microscopy.

Quantitative detection of human DNA in rat spinal cord tissue using Alu sequence

Animals were sacrificed at 24 hours or 4 weeks post-transplantation. Spinal cord sections up to 1 cm caudal and rostral of the lesion epicenter were harvested after PBS perfusions and small pieces of tissue were placed in autoclaved 1.5 mL microfuge tubes. DNA was extracted using DNeasy Blood & Tissue Kit (Qiagen# 69504) according to manufacturer's protocol. In short, 200-300 µL of extraction buffer was added and the tissue was homogenized using a sterile blue pestle. Additional extraction buffer was added until the total volume was 500 µL. Fifty microliters of Proteinase-K solution (10 mg/mL) was added to the tube and mixed. Tubes were then incubated at 55 °C for 2 hours with occasional vigorous mixing until the samples were homogeneous, non-viscous fluids. 700-800 µL of PCI (phenol: chloroform: IAA) was added. The samples were then vortexed briefly and centrifuged for 3-5 minutes at 12,000 rpm. Four hundred to 500 µL of the aqueous layer for each sample was collected without disturbing the interface or PCI layers. Forty to 50 µL of 3M NaAC, pH 5.3, was added to each tube and mixed. The tubes were cooled at −80 °C for 10 minutes to precipitate the DNA and then pelleted by centrifugation at 12,000 rpm for 2-20 minutes at 4 °C. Supernatant was aspirated and 1.0 mL of 70-80% ethanol was added. The pellets were washed with ethanol for 20 minutes at 4 °C without agitation. The pellets were then spun at 12,000 rpm for 3-5 minutes and the ethanol was aspirated. The samples were then dried for 5-30 minutes at room temperature before the pellet was resuspended in 100-300 µL of TE solution. Alu element presence was then detected and quantified using qPCR.

The genomic DNA mass per primary human cell was estimated by first calculating the total number of base pairs in a diploid human genome (6×10^9), derived from the 3×10^9 base pairs in the haploid genome. This figure was then multiplied by the average weight of a base pair (660 Da) and the weight of a dalton (1.67×10^{-12} pg), yielding an estimated 6.6 pg of DNA per diploid cell, which is roughly the same as found previously.[28]

For the detection of human DNA within rat spinal cord tissue, a qRT-PCR was performed using an Applied Biosystems 7900HT Fast Real-Time PCR System and SYBR Green Real-Time PCR Master Mixes. Human-specific primers targeting an Alu sequence (forward: 5′-CACCTGTAATCCCAGCACTTT-3′, reverse: 5′-CCCAGGCTGGAGTGCAGT-3′) were employed.[29] The PCR protocol included an initial denaturation at 95 °C for 5 minutes, followed by 40 cycles of denaturation at 95 °C for 10 seconds, annealing at 65.35 °C for 110 seconds, and extension at 72 °C for 10 minutes. To quantify human DNA, standard curves were generated using serial dilutions of human DNA in rodent-specific DNA. The total DNA content was determined using primers for rodent gene B1 elements (forward: 5′-ACGCCTTTAATCCCAGCACTC-3′, reverse: 5′-GAACTCACTCTGTAGACCAGGCTG-3′), which amplify a sequence of 80-83 base pairs, in contrast to the 234-250 base pair length of the Alu sequence amplified.[30]

Nuclear extraction for bulk RNA sequencing

Nuclei were isolated from PFA-fixed cryoprotected tissue and the nuclei of hiPSC-NPCs were sorted for using fluorescent activated nuclear sorting (FANS) for GFP expression, after which total RNA was extracted. Three rRNA-depleted stranded libraries were generated for each condition of immunosuppressant and immunodeficient animals using the extracted RNA, which were then multiplexed. Paired-end 100 bp sequencing was performed using an Illumina NextSeq 550 sequencer. The raw sequence reads were aligned using TopHat to the hg19 UCSC human reference genome. FASTQ files were The Illumina Truseq adapters from FASTQ files were trimmed with Trim Galore.

Differential gene expression analysis

The raw gene expression counts were processed using the edgeR package in R (version 4.4.1) for differential gene expression (DGE) analysis. The input data consisted of raw count values. An exact test was performed using the exactTest function to identify differences between the experimental and control groups. Log fold-change (FC) values were calculated as the ratio of experimental to control conditions (log2 scale). Significant genes were identified using a false discovery rate (FDR) threshold of 0.1.

For principal component analysis (PCA), a multidimensional scaling (MDS) plot was generated using the plotMDS function to visualize the overall variation between the control and experimental groups.

Gene ontology analysis

Differentially expressed genes (DEGs) were analyzed using the g:GOSt functional profiling tool in gProfiler (version February 12, 2024) to identify enriched Gene Ontology (GO) terms, pathways, and functional categories. The analysis was conducted using species-specific settings for *Homo sapiens*, and statistical significance was determined with the default algorithm for multiple testing correction. To refine and reduce redundancy in the enriched GO terms, we employed REVIGO (version 1.8.1), applying the "medium similarity" threshold, which retains only functionally distinct and statistically significant GO terms. The reduced set of GO terms was exported in a Cytoscape-compatible file format and subsequently imported into Cytoscape (version 3.10.1) for network visualization. During visualization, we manually inspected the network to remove redundant or irrelevant nodes, ensuring the final network retained only biologically meaningful connections. Node sizes were adjusted based on the significance of the GO terms (adjusted *P*-value), and edge thickness was scaled to reflect the strength of relationships between terms. The finalized network was exported in GraphML format and imported into R (version 4.4.1) for further graph analysis using the igraph package. Custom network plots were generated to display nodes representing enriched GO terms, with edges indicating relationships based

on similarity scores. The size of the nodes was proportional to their significance, while edges reflected the similarity between GO terms, providing an informative visualization of the GO term relationships.

Cell type deconvolution with BayesPrism

We utilized the single-cell RNA sequencing dataset of the human developing spinal cord (GSE188516)[31] for our analysis. The CellRanger outputs were downloaded and processed using the Seurat[32] package in R. Cells with fewer than 200 features or features expressed in fewer than 3 cells were filtered out. Gene identifiers were converted from Ensembl IDs to HGNC symbols using the biomaRt package.[33] Genes without corresponding HGNC symbols or with non-unique mappings were excluded. The data were normalized in Seurat, and duplicated genes were removed. We applied the BayesPrism tool[34] to deconvolute the bulk RNA sequencing data using the single-cell reference data. BayesPrism utilizes a Bayesian framework to estimate both the proportion of different cell types within a bulk sample (cell fractions) and the gene expression levels specific to each cell type.

Stereological quantification of cell survival

The evaluation of cell survival following NPC transplantation was carried out on serial axial sections of the spinal cord (spaced at 240 µm). This distance was used to avoid over-counting. We undertook a statistically unbiased method to determine the survival of NPC transplants ($n = 3$). Using a Leica fluorescent microscope with 25 × main objective, we traced the transplant region in each cross section. Using Stereo Investigator, a set of systematic random samples measuring 200 × 200 mm in area were generated. The software's optical fractionator sampling probe was used for workflow creation and sampling design. Next, we counted the number of GFP + NPCs containing a nucleus (GFP/DAPI positive cells) in each given field, and the average density (in cells per cubic millimeter) for each field was calculated. The total number of surviving GFP^+ cells was then estimated by multiplying the mean average density by the transplant volume in each rat.

Statistics

All quantitative data were expressed as mean ± SEM. Differences between groups were assessed using one- or two-way analysis of variance (ANOVA) with Bonferroni or Tukey's post hoc test to correct for multiple comparisons. The normality assumption was tested using the Shapiro-Wilk test. The equality of the probability distributions was assessed using a *Z*-score, and the results were visually confirmed by plotting a scatterplot to assess linearity. The results were considered statistically significant if $P < .05$. Data were analyzed using GraphPad Prism (version 10.2.3) or R (version 4.4.2).

Results

Differential survival of NPCs in Wistar, RNU, and X-SCID rats

To investigate the impact of different immune environments on the survival and integration of transplanted human iPSC-derived neural progenitor cells (hiPSC-NPCs), we utilized 3 distinct rat models: wild-type Wistar rats, T-cell deficient Rowett Nude (RNU) rats, and severely immunodeficient X-linked severe combined immunodeficiency (X-SCID) rats. We quantitatively assessed the survival of transplanted hiPSC-NPCs at two time points: 1 day and 4 weeks post-transplantation. At 1 day post-transplantation no significant differences were observed in the number of surviving human cells among the three rat models (Wistar, RNU, and X-SCID) (Figure 1A). This suggests that the immediate post-transplantation survival is comparable across these different immune environments, likely before significant immune responses are mounted. However, at 4 weeks post-transplantation, marked differences in NPC survival became evident. X-SCID rats exhibited significantly higher retention of transplanted NPCs compared to both Wistar ($P < .01$) and RNU rats ($P < .01$) (Figure 1B). The survival in X-SCID rats was approximately double that observed in RNU rats, which in turn showed higher survival than Wistar rats. This hierarchy of survival (X-SCID > RNU > Wistar) correlates inversely with the degree of immunocompetence of each model. Interestingly, while Wistar and RNU rats showed a decline in cell numbers over this period, X-SCID rats maintained a relatively stable population of transplanted cells. The difference between day 1 and week 4 cell counts in X-SCID rats was not statistically significant (n.s.), suggesting minimal cell loss in this highly immunodeficient environment (Supplimentary Figure S1).

To corroborate our quantitative PCR-based cell counting, we performed stereological analysis of transplanted cell survival at 4 weeks post-transplantation (Figure 1C, D). This analysis confirmed the trend observed in our molecular quantification, with X-SCID rats showing significantly higher numbers of surviving cells compared to both RNU ($P < .01$) and Wistar ($P < .01$) rats. These immunostaining for human nuclear antigen (hNuA) revealed larger and more robust grafts in X-SCID rats compared to RNU rats, with minimal survival evident in Wistar rats. These results collectively demonstrate that the degree of host immunodeficiency significantly impacts the survival of transplanted hiPSC-NPCs in a rodent SCI model. The superior survival observed in X-SCID rats, which lack both T and B cells, suggests that both arms of the adaptive immune system play crucial roles in the rejection of xenografted human NPCs. The intermediate survival in RNU rats, deficient only in T cells, indicates that while T cells are major mediators of xenograft rejection, B cells also contribute to this process. The poor survival in immunocompetent Wistar rats underscores the challenges faced in translating cell therapies to immunocompetent hosts without effective immunomodulation strategies.

Human PBMC infusion in RNU rats leads to reduced survival of transplanted NPCs due to allogenic immune recognition

To investigate the role of human immune cells in the survival of transplanted human iPSC-derived neural progenitor cells hiPSC-NPCs, we developed a humanized RNU rat model by infusing human peripheral blood mononuclear cells (PBMCs) into RNU rats prior to NPC transplantation. This model simulates a human-like immune response in the context of SCI.

We compared outcomes in RNU rats and humanized-RNU rats to evaluate the influence of different immune environments on the survival of transplanted hiPSC-NPCs. CD3 immunohistochemical staining of spinal cord tissue from both groups at 4 weeks post-transplantation revealed a contrasting difference in immune cell infiltration (Figure 2A). RNU rats showed minimal CD3-positive staining, indicating a lack of T cell infiltration due to the absence of functional T cells, which provides a permissive environment for the survival of transplanted human NPCs. In contrast, humanized-RNU

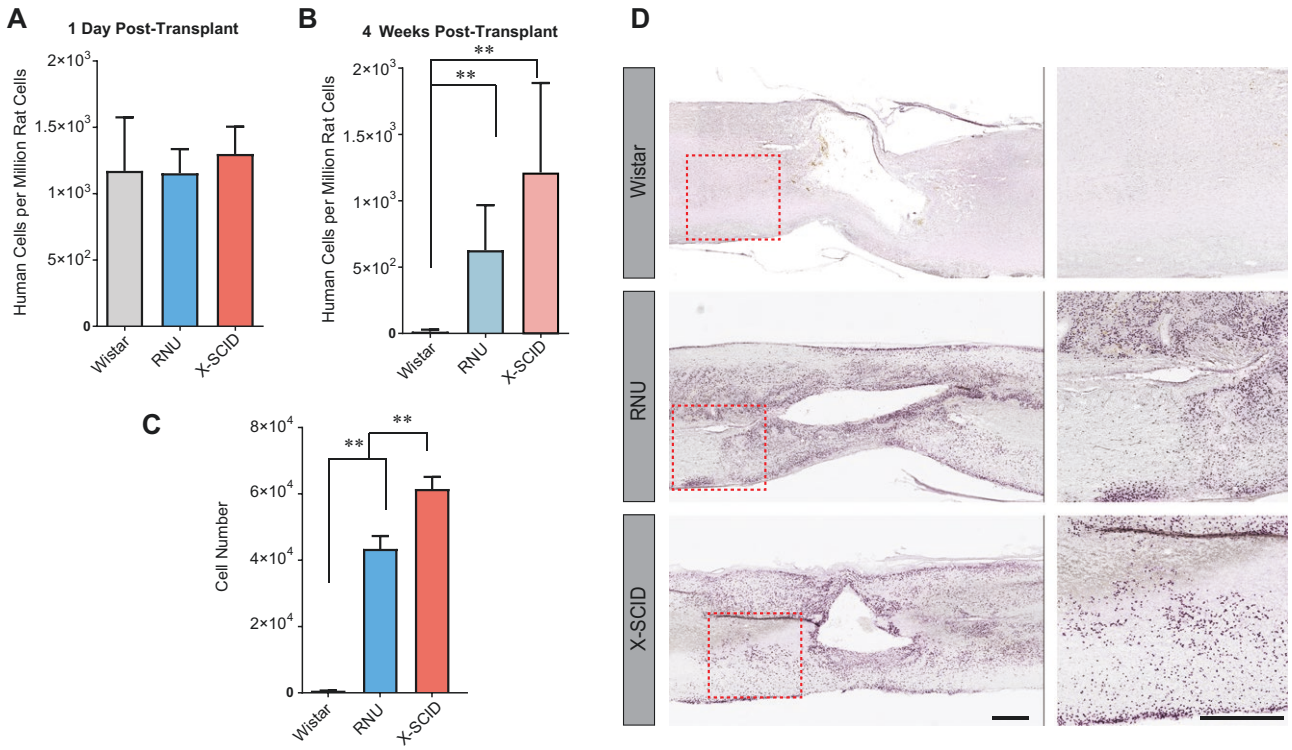

Figure 1. Comparison of transplanted cell survival in RNU rats and X-SCID rats. 200,000 wild-type hNPCs were transplanted 2 weeks post-injury into the parenchyma of rat spinal cords. Genomic DNA was isolated from a 20-mm section of a harvested spinal cord, and Alu elements were quantified using real time qPCR for surviving grafted cell extrapolation. (A) There were no significant differences in number of grafted cells found between all treatments when rats were sacrificed 1-day post-transplant ($n = 3$) where a one-way ANOVA was performed. (B) At 4 weeks post-transplant, X-SCID rats exhibited significantly higher rates of graft cell survival than the Wistar control (one-way ANOVA with Tukey's multiple comparison test; $^{**}P < .05$), and approximately double the survival compared to RNU rats. (C, D) Immunostaining of rat tissue sections was performed 4 weeks after NPC transplantation ($n = 3$), using the anti-human nuclear antigen (hNucA) to specifically mark human cells. (C) The quantification of cells positive for hNucA was used to estimate the number of human cells in each group 4 weeks post transplant, with significant differences found between all groups. (D) hNuCA DAB staining of Wistars, RNU, and X-SCID rat spinal cord tissue that received transplanted hNPCs 2 weeks post injury and were sacrificed 4 weeks post transplant. Scale bar = 500 μm.

rats exhibited significant CD3-positive staining, particularly around the injury epicenter, demonstrating substantial T-cell infiltration. This suggests a robust immune response akin to the human immune environment, leading to increased immune-mediated cell loss.

To assess the effect of human immune cell presence on transplanted NPC survival, we quantified the number of surviving human cells in both RNU and humanized-RNU rats at four weeks post-transplantation using Alu element qPCR (Figure 2B). The results revealed a significant reduction ($P < .05$, unpaired t-test) in the number of surviving transplanted human cells in humanized-RNU rats compared to regular RNU rats. Specifically, humanized-RNU rats showed approximately a 50% reduction in surviving human cells per million rat cells compared to regular RNU rats (627.2 ± 132 vs. 324 ± 67 human cells per million rat cells, mean ± SEM). This marked decrease in NPC survival in the presence of human immune cells suggests that the transplanted human NPCs were recognized as allogenic by the infiltrated human immune cells, leading to their elimination.

Immunosuppressive agents enhance NPC retention in Wistar rats but exhibit adverse effects on host health

Next, we tested the efficacy of immunosuppressive agents—Cyclosporine A (CsA), Tacrolimus (FK506), and Mycophenolate Mofetil (MMF)—on enhancing NPC viability in Wistar rats.

CsA and FK506 suppress T-cell activation and proliferation by inhibiting the calcineurin NF-AT pathway.[35] These two immunosuppressants inhibit calcineurin activation through targeting immunophilins, but Tacrolimus has been shown to be more efficient than CsA.[36,37] Conversely, Mycophenolate Mofetil disrupts the de novo synthesis of guanosine nucleotides in T and B cells, hindering their activation, proliferation, and differentiation.[38] Consequently, these pharmacologically suppressed B and T cells may interact differently with grafted NPCs as compared to non-suppressed counterparts. Furthermore, it is crucial to consider the potential direct impact of these immunosuppressants on NPC gene expression and differentiation during analysis.

We checked the impact of these pharmacological immunosuppressants on transplanted human NPC survival and retention in Wistar rats. On day one post-transplantation, no significant differences were observed in NPC retention among the CsA, FK506, and MMF treatment groups, or the non-immunosuppressed control group. This suggests either an initial tolerance or a lack of immediate immune response to the transplanted cells (Figure 3A). However, after 4 weeks, a marked divergence in cell survival/retention became evident. The non-immunosuppressed group exhibited minimal NPC retention, while groups treated with

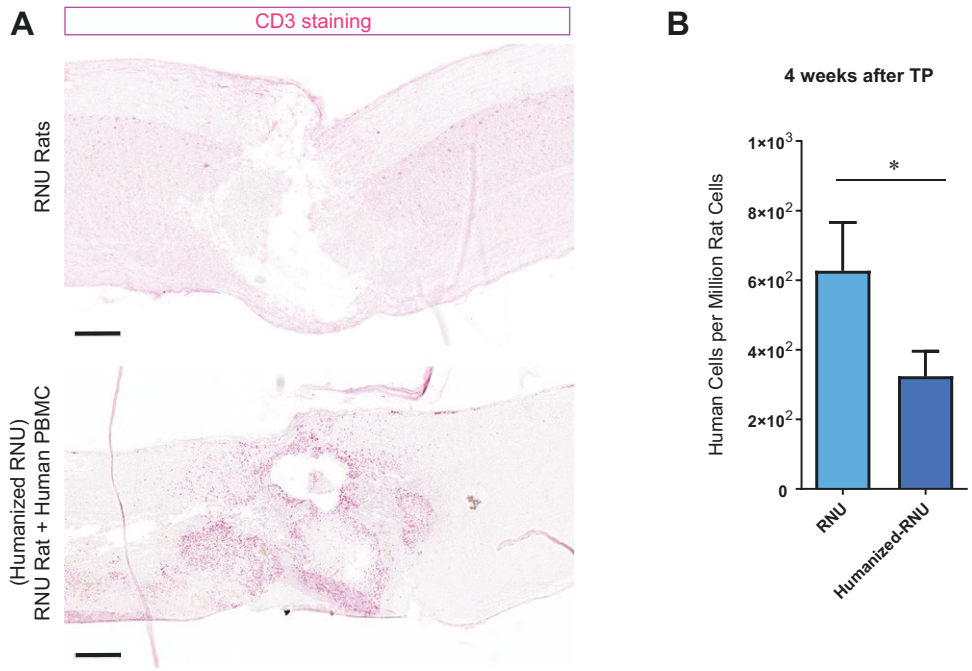

Figure 2. (A) Histological analysis of RNU rat spinal cord tissue with T-cell marker, CD3, at 4 weeks following NPC transplantation. The upper panel displays a section from a control RNU rat. The lower panel exhibits spinal cord tissue from RNU rats infused with human PBMCs. Scale bars = 400 μm. (B) Quantitative analysis of human cell engraftment in the spinal cords of RNU rats 4 weeks post-transplantation ($P < .05$).

immunosuppressants displayed significantly higher NPC survival. Notably, the FK506-treated group exhibited the highest NPC retention, suggesting a potentially more favorable environment for NPC survival and proliferation (Figure 3B-D). Despite the effectiveness of FK506 in enhancing the survival of transplanted human NPCs post-transplantation, it is crucial to note the adverse effects observed in the rat subjects. Administration of FK506 was associated with severe dermatological complications, including pronounced skin lesions on the dorsal surface, increased skin rigidity, and dryness. These symptoms were exacerbated by secondary bacterial and fungal infections, aggravating the severity of the lesions. Furthermore, there was a noticeable decline in the overall health and vitality of the rats, characterized by reduced mobility and general weakness, culminating in a significantly decreased survival rate among the rat cohort, primarily due to the infectious complications.

Gene expression profiling of NPCs post-transplantation in SCI models

To elucidate the changes in gene expression of NPCs following transplantation into SCI models, and to assess the impact of immune cell infiltration, particularly T-cells and B-cells, we isolated spinal cord tissue, performed nuclear extraction, and isolated the nuclei of transplanted NPCs. Utilizing fluorescent-assisted nuclear sorting (FANS), we purified GFP-positive human cells and subsequently isolated RNA from these cells for RNA sequencing.

Differential gene expression analysis was first performed across the various conditions, revealing substantial differences in transcriptional activity. As shown in the volcano plots (Figure 4A), the magnitude and significance of these changes were variable across different immunological contexts. In the RNU rats, 7480 significant differentially expressed genes (DEGs) were identified, with upregulation of genes associated with neuronal differentiation (*ASCL1*, *DCX*) and glial markers (*GFAP*, *CNP*), suggesting a neural-supportive environment. Similarly, X-SCID rats displayed 8082 DEGs, also marked by the expression of both neural and glial markers. In contrast, Tacrolimus-treated Wistar rats exhibited 2734 significant DEGs, with an enrichment in NPC survival markers such as *VGF* and *NFASC*, and a reduction in stress-related gene expression. Cyclosporin A-treated rats showed 2171 DEGs, whereas Mycophenolate Mofetil-treated animals displayed 2841 DEGs (Figure 4A).

To further investigate the global transcriptional changes in NPCs under these different immune conditions, principal component analysis (PCA) was performed (Figure 4B). This analysis revealed clear clustering of transcriptomic signatures according to each treatment group. NPCs transplanted into RNU and X-SCID rats exhibited substantial transcriptional overlap, suggesting a shared response to the absence of immune rejection in these immunodeficient models. In contrast, NPCs from Wistar rats treated with immunosuppressants (Cyclosporin A, Tacrolimus, and Mycophenolate Mofetil) formed distinct clusters, indicating that immune modulation through pharmacological means elicited unique gene expression patterns. Interestingly, NPCs transplanted into humanized RNU rats (RNU + PBMC) displayed a completely distinct transcriptional signature, likely reflecting the presence of human B and T cells in the host. This allogeneic immune response likely contributed to the altered gene expression profile, illustrating a regulated interaction between the humanized immune system and the grafted NPCs.

To provide more detailed insights into immune-related transcriptional changes, heatmap analysis was employed to visualize the differential expression of immune-related genes, including B- and T-cell markers (Figure 4C). As expected,

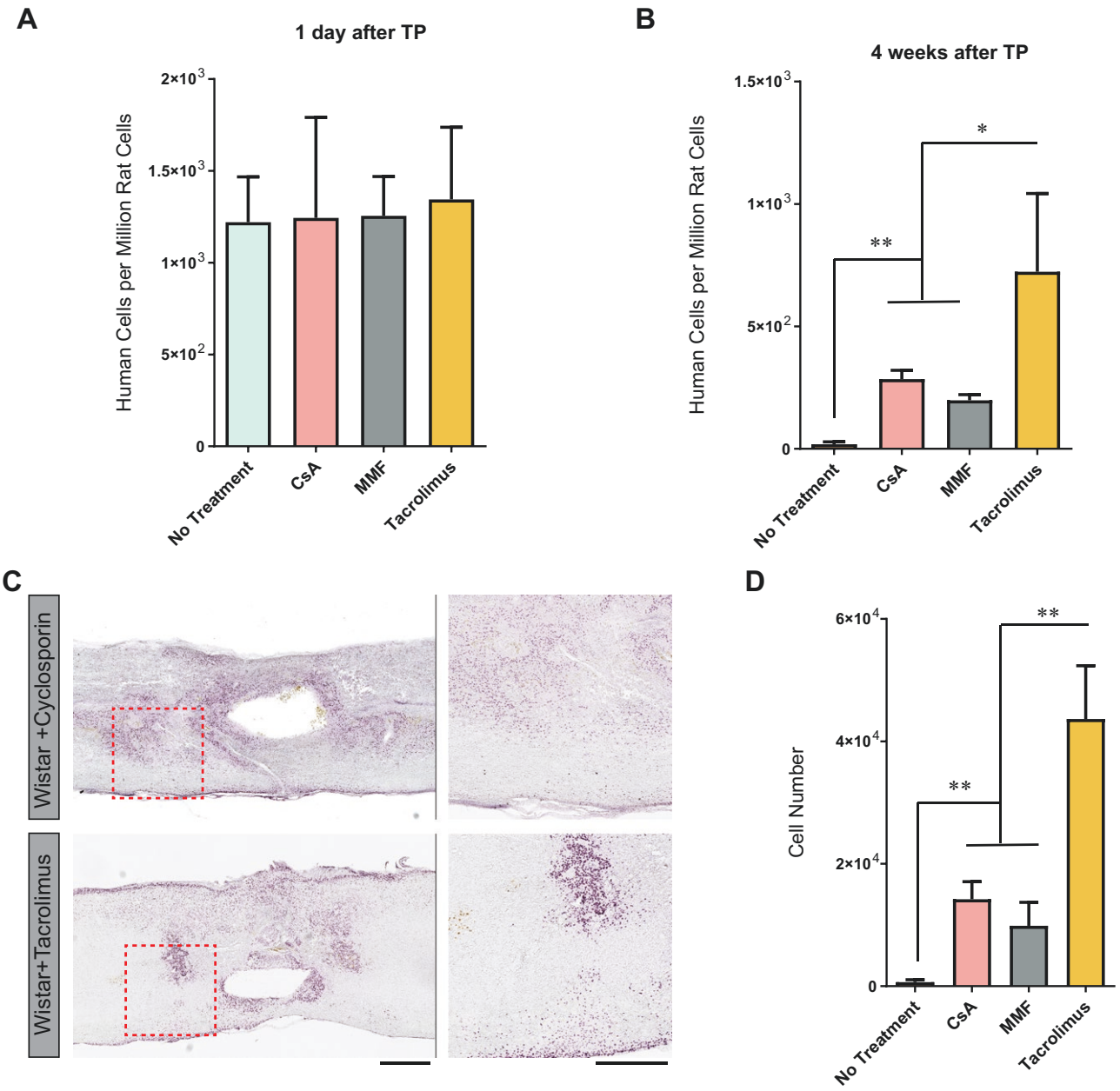

Figure 3. Wistar rats were treated with a pharmacologic immunosuppressive agent or no treatment and were transplanted with NPCs 2 weeks post-injury ($n = 6$). Genomic DNA was isolated from a 20-mm section of the harvested spinal cord, and Alu elements were quantified using real-time qPCR for total surviving grafted cell extrapolation. (A) There were no significant differences found between all treatments when rats were sacrificed 1-day post-transplant ($n = 3$, $P < .05$). (B) Rats were sacrificed 4 weeks post-transplant. NPC graft survival was highest in Tacrolimus treated Wistar rats and in RNU rats, exceeding both CsA and MMF treatments at a statistically significant level. To analyse the data, we performed 2-way ANOVAs with Bonferroni post hoc corrections ($n = 3$, $P < .05$). (C) Rats from each immunosuppressive agent group were sacrificed and their spinal cords were extracted 4 weeks post-NPC transplantation. Tissue sections were stained with mouse anti-human nuclear antigen and visualized using anti-mouse HRP. Scale bars = 500 μm. (D) Cell counts for grafted human cells from each immunosuppressant group's immunohistochemistry images are compared.

humanized RNU rats exhibited the highest expression of these immune-related genes, consistent with the activation of an adaptive immune response mediated by human immune cells. In contrast, RNU and X-SCID rats, being immunodeficient, showed much lower expression of these immune-related genes. This pattern underscores the differential involvement of immune cells in each model and the profound influence that immune context has on NPC behavior and survival.

Our differential gene expression analysis highlighted significant alterations in the gene expression profiles of transplanted NPCs across different immune environments (Figure 4C), particularly in pathways related to immune response, cell survival, and neural differentiation. These findings underscore the complex interplay between transplanted NPCs and the host immune environment, offering insights into the mechanistic underpinnings of NPC behavior in different immunological contexts. Such information is critical for optimizing NPC-based therapeutic strategies for SCI, ensuring enhanced survival, integration, and functional efficacy of transplanted cells.

Comparing NPCs transplanted in genetic immunodeficient RNU and X-SCID rats, and those treated with

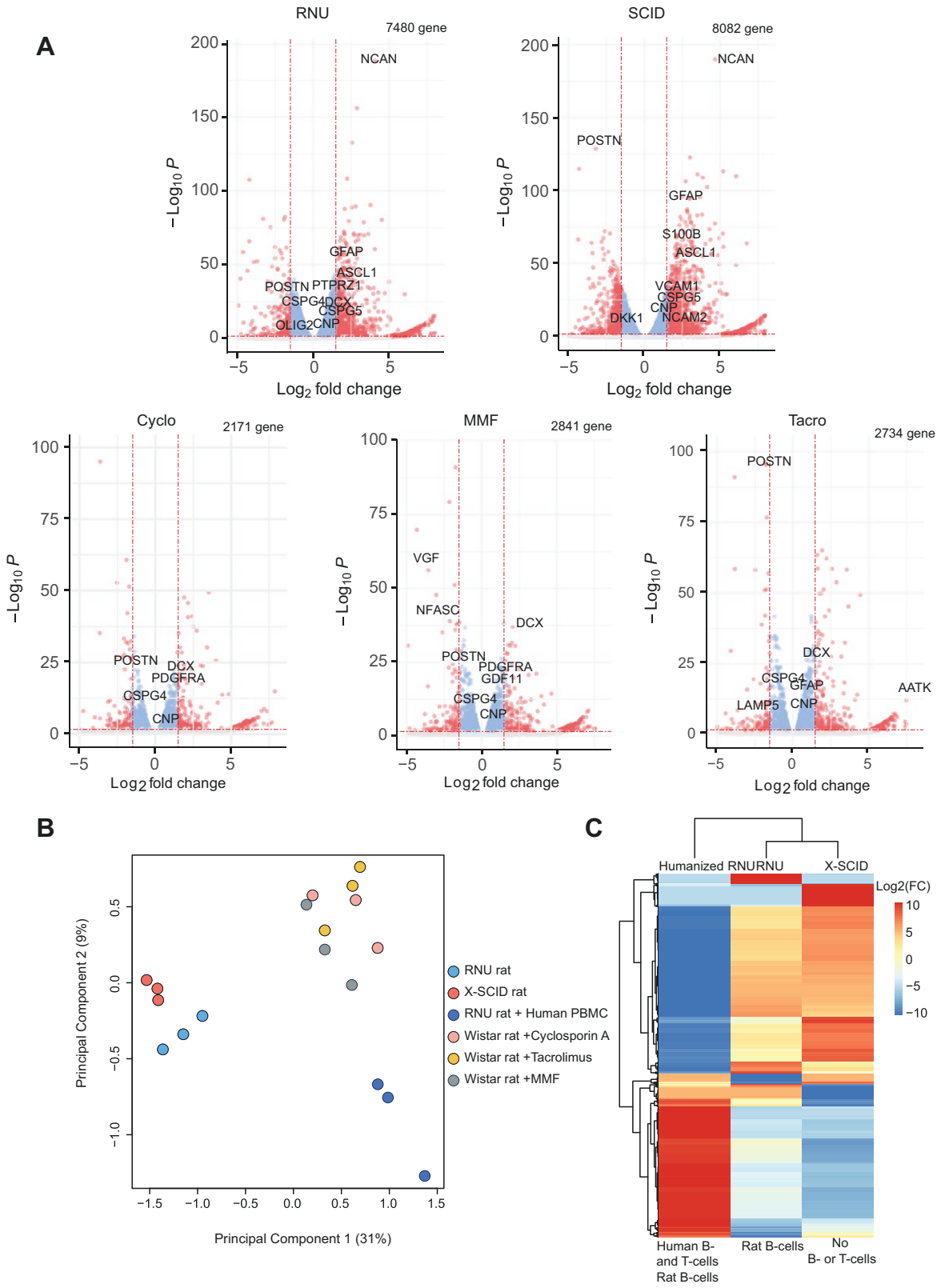

Figure 4. (A) Volcano plots depicting the number of significantly differentially expressed genes (DEGs) (adjusted *P*-value < .05, log2 fold change ≥ |1|) across the various immunological environments: RNU, SCID, Tacrolimus (Tacro), Cyclosporin A (Cyclo), and Mycophenolate Mofetil (MMF). The *x*-axis represents the log2 fold change, indicating the magnitude of gene expression differences between transplanted NPCs in each treatment condition compared to a baseline, while the *y*-axis shows the −log10 of the adjusted *P*-value, reflecting the statistical significance of these differences. Each plot is labelled with the number of significant DEGs identified under each condition. (B) Principal component analysis (PCA) of RNA-sequencing data derived from NPCs post-transplantation. RNU rats (blue circles) and X-SCID rats (red circles) show overlapping clusters. Wistar rats treated with Cyclosporin A (pink circles), Tacrolimus (yellow circles) and Mycophenolate Mofetil (grey circles) also form a tight cluster. (C) Heatmap with hierarchical clustering of differential gene expression in NPCs across different rat models. The heatmap visualizes log2 fold changes (Log2(FC)) in gene expression compared to the Tacrolimus-treated group.

immunosuppressants CsA, Tacrolimus, and MMF, we observed distinct expression profiles. Although the DGE profiles in the immunosuppressant-treated group were more similar to each other, they differed markedly from those in RNU and X-SCID groups. Interestingly, RNU and X-SCID groups exhibited more similar expression profiles to each other. This suggests differential immune responses affecting NPC behavior.

Significant upregulation was observed in genes related to neurogenesis, synaptic plasticity, and neuronal differentiation in the immunodeficient rat breeds (Figure 5A). Hierarchical clustering of the DGE data revealed distinct clusters. A notable cluster (red cluster) differed significantly between RNU and X-SCID rats, predominantly in genes involved in "neurogenesis," "nervous system development," and "neuron development," which were more pronounced in the X-SCID rat group (Figure 5B).

In another cluster (Green Cluster), observed in both RNU and X-SCID rats compared to those treated with immunosuppressants, genes related to "neural tube development," "neuron projection development," and "neurogenesis" were more pronounced. This indicates that B-cells and T-cells might inhibit differentiation into neurons. Conversely, a distinct cluster (Blue Cluster) was prominent in rats treated with immunosuppressants, suggesting these agents might induce stress and potential DNA damage in transplanted NPCs.

The data also highlighted a significant response to immune cell infiltration. We observed upregulation of genes involved in immune response and inflammation, indicating an active interplay between transplanted NPCs and the host immune system. Specifically, differential expression of genes related to T- and B-cell signaling pathways suggests a complex mechanism of interaction between NPCs and these immune cells, impacting NPC behavior and fate post-transplantation.

Gene set enrichment analysis and pathway mapping

Upon close examination of the RNAseq data and correlating it with gene sets related to NPCs, neurons, astrocytes, and oligodendrocyte differentiation, further analysis using

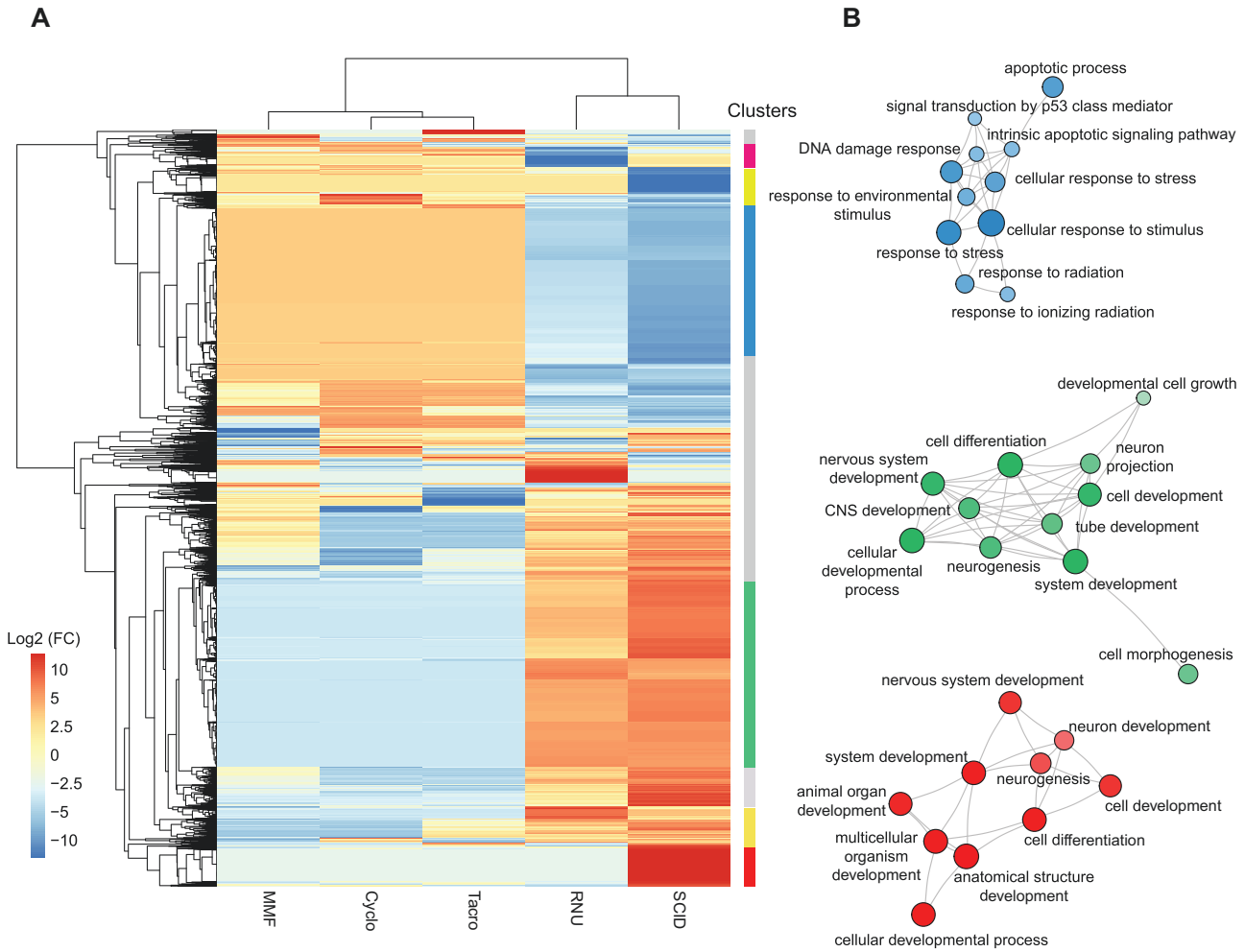

Figure 5. (A) Heatmap and hierarchical clustering showing the significantly differentially expressed genes (FDR < 0.05) in NPCs transplanted into RNU rats, X-SCID rats, or Wistar rats treated with immunosuppressants (MMF, CsA, or Tacrolimus). The differential gene expression (DGE) is compared with that in NPCs transplanted into RNU rats and subsequently injected with human PBMCs. Data are presented on a log2 scale. Major clusters are indicated by color codes on the right side of the heatmap. (B) An interactive network showing the relationships between enriched GO terms for biological processes. The significant ($P < .05$) biological processes GO terms for the blue, green, and red clusters were simplified into the most representative terms by REVIGO, based on their semantic similarity.

Gene Set Enrichment Analysis (GSEA) and pathway mapping tools revealed that several key pathways were significantly impacted. These included pathways related to neuro-immunomodulation, cell survival, and cellular stress response. The data suggest that the transplanted NPCs not only adapt to the SCI environment but also actively participate in modulating the immune response, potentially influencing the regenerative process (Figure 6).

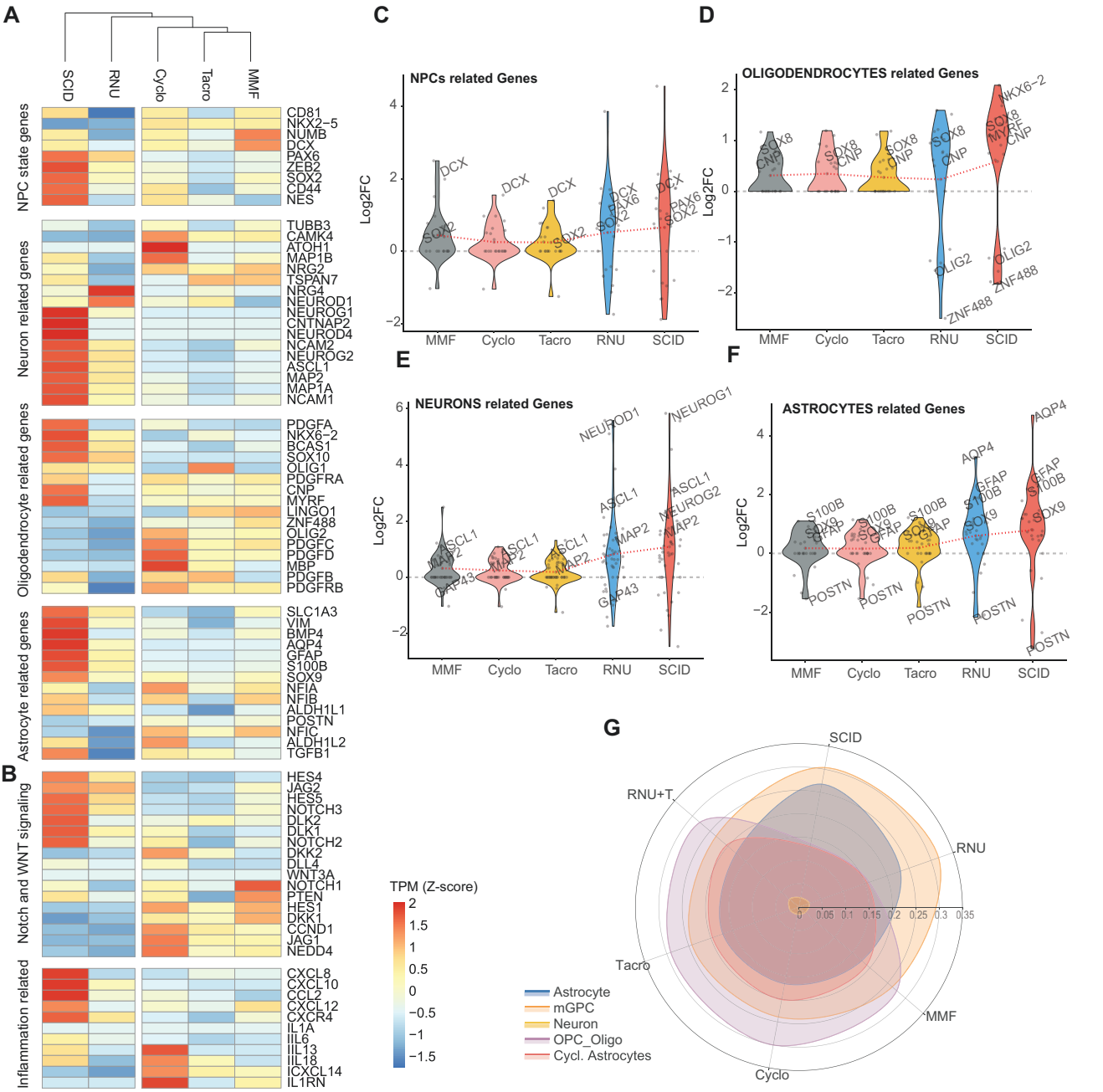

Figure 6. (A) Heatmap illustrating gene expression profiles in differentiated cells from transplanted NPC across various treatment groups (MMF, Cyclo, Tacro, RNU, X-SCID). This heatmap categorizes genes based on cell-type specificity: NPC-state genes, neuron-related genes, oligodendrocyte-related genes, and astrocyte-related genes. Gene expression levels are normalized and presented as transcripts per million (TPM) z scores, with a color gradient ranging from red (high expression) to blue (low expression). (B) Heatmap depicting the gene expression patterns associated with key developmental pathways, notably Notch and WNT, and inflammation-related genes in the same treatment cohorts as in (A). This visualization aids in discerning the differential gene activation within these critical signalling pathways under varied treatment conditions. (C-F) Visualization of variations in gene expression specific to NPCs, neurons, oligodendrocytes, and astrocytes using violin plots. These plots illustrate the distribution of log-transformed fold changes (Log2FC) in gene expression across the different treatment groups, highlighting the diverse expression patterns under each treatment condition. Grey dashed lines denote the thresholds for gene upregulation (above zero) and downregulation (below zero). A red dotted line connects the average Log2FC values for each treatment group, providing an overview of the mean expression changes across the gene categories. G) The radar plot illustrates the averaged proportions of various cell types in bulk RNA-seq samples, deconvoluted using BayesPrism with the Anderson et al. single-cell dataset 31. The plot displays the proportions of five major cell types: Astrocytes (blue), multipotent glial progenitor cells (mGPCs, orange), Neurons (yellow), oligodendrocyte progenitor cells and oligodendrocytes (OPC_Oligo, purple), and cycling astrocytes (red). Each spoke represents a different immunomodulation. The radial axis indicates the proportion of each cell type, ranging from 0 at the center to 0.35 at the outer edge.

In both RNU and X-SCID rats, the transplanted grafted human cells exhibited increased expression of neuronal genes. Interestingly, NEUROG1 was significantly upregulated in X-SCID rats, while in RNU rats, NEUROD1 was significantly upregulated.

Furthermore, the NPCs in both models demonstrated a significant increase in the expression of astrocytic-related genes, such as GFAP and S100B, coupled with a downregulation of oligodendrocyte lineage-related genes like OLIG2 and ZNF488 (Figure 6).

Notably, in X-SCID rats compared to RNU, there was a significant upregulation of genes associated with neuronal differentiation, such as ASCL1, NEUROGD4, and NEUROG1, indicating a tendency toward neuronal lineage commitment. This suggests that the host's immune system plays a critical role in directing the fate of transplanted NPCs. Additionally, transcriptomic analysis revealed increased expression of genes associated with anti-inflammatory pathways in both RNU and X-SCID rats, which could be attributed to the interaction between the NPCs and the host's immune cells.

Analyzing our RNA-seq data using deconvolution and the BayesPrism method with the Anderson et al. (2023) single-cell RNA-seq dataset[31] revealed that different immunodeficient backgrounds and immunosuppressive treatments distinctly affect the cellular composition of xenografted spinal cord tissue. Our analysis revealed distinct cellular profiles associated with immunodeficient backgrounds and immunosuppressive treatments. In immunodeficient conditions (RNU and SCID), we observed a marked increase in multipotent glial progenitor cells (mGPCs), with proportions reaching up to 31.9% in RNU and 31.8% in SCID, compared to 23.3%-24.3% in immunosuppressed conditions. This suggests that immunodeficient environments may foster the maintenance of a more progenitor-like state. Concurrently, mature astrocytes showed higher prevalence in these immunodeficient conditions, with proportions of 22.0%-24.7% in RNU and 26.2%-27.4% in SCID, versus 16.5%-18.5% in immunosuppressed conditions. This finding indicates potential acceleration of astrocytic differentiation or enhanced maintenance of mature astrocytes in immunodeficient hosts.

In contrast, immunosuppressive treatments (RNU + T, Tacro, Cyclo, and MMF) demonstrated a notable shift towards oligodendroglial lineages. The combined oligodendrocyte progenitor cell and oligodendrocyte (OPC_Oligo) population exhibited substantial increases under these conditions, with proportions ranging from 26.2%-31.1%, compared to 13.1%-17.5% in immunodeficient conditions. This suggests that immunosuppressive regimens may promote oligodendroglial lineage progression or maintenance, potentially influencing myelination processes in the xenografted tissue.

Interestingly, we observed a slight but consistent increase in cycling astrocytes under immunosuppressive conditions. Their proportions ranged from 18.6%-20.7% in treated groups, compared to 12.8%-16.0% in immunodeficient conditions. This finding potentially indicates enhanced astrocyte turnover or gliogenesis in response to immunosuppressive therapies, which could have implications for tissue homeostasis and repair processes.

Neurons consistently showed low proportions across all conditions (1.0%-2.8%), reflecting the typically high glial-to-neuron ratio in spinal cord tissue. This stability suggests that neither immunodeficiency nor immunosuppression substantially altered the neuronal component of the xenografted tissue within the observed timeframe.

Discussion

In this study, we investigated the complex interplay between the host immune system and transplanted human iPSC-derived neural progenitor cells (hiPSC-NPCs) in spinal cord injury (SCI) models. Our findings reveal critical insights into how the immune environment shapes the survival, gene expression, and differentiation of transplanted NPCs, with significant implications for cell-based therapies in SCI.

Differential NPC survival and its implications

Our results demonstrated a clear hierarchy of NPC survival (X-SCID > RNU > Wistar) that inversely correlated with the degree of host immunocompetence. This finding aligns with previous studies showing enhanced graft survival in immunodeficient hosts.[23,24] However, while increased survival is often considered beneficial, our transcriptomic analysis reveals that the absence of immune cells may significantly alter the behavior and fate of transplanted NPCs.

Transcriptomic alterations in different immune environments

Our gene expression analysis revealed distinct transcriptomic signatures across different immune environments. Notably, NPCs in immunodeficient hosts (RNU and X-SCID) exhibited upregulation of genes associated with neurogenesis and synaptic plasticity, such as NEUROG1, NEUROD1, and ASCL1. This finding suggests that the absence of adaptive immune responses creates a permissive environment for neuronal differentiation.

However, this apparently favorable gene expression profile must be interpreted cautiously. The lack of normal immune cell interactions in these models may result in an artificial environment that does not reflect the complex signaling milieu of an immunocompetent host. As demonstrated by Ziv et al,[25] immune cells, particularly T cells, play crucial roles in supporting neurogenesis and cognitive function under normal conditions. Thus, the increased expression of neurogenic genes in immunodeficient models may not necessarily translate to improved functional outcomes.

Immune cell-NPC interactions and their impact on gene expression

In immunocompetent Wistar rats, we observed a different gene expression profile in transplanted NPCs, characterized by upregulation of genes related to immune modulation, stress response, and glial differentiation. This finding underscores the significant impact of immune cell-NPC interactions on gene expression.

Immune cells, through the production of cytokines and other signaling molecules, can profoundly influence NPC fate. For instance, our data showed increased expression of GFAP and S100B in NPCs transplanted into Wistar rats, indicating a bias toward astrocytic differentiation. This aligns with previous studies showing that pro-inflammatory cytokines like IL-1β and TNF-α can promote astrogliogenesis.[39]

Conversely, in immunodeficient rats, we observed downregulation of genes associated with oligodendrocyte differentiation, such as OLIG2 and ZNF488. This finding

is particularly intriguing as it suggests that normal immune function may be necessary for promoting oligodendrogenesis. Indeed, recent research has shown that certain T-cell subsets can support oligodendrocyte differentiation and myelination.[40]

Transcription factor dynamics and cell fate decisions

The altered expression of key transcription factors in different immune environments provides mechanistic insight into how immune cells influence NPC fate decisions. In immunodeficient rats, we observed upregulation of neuronal transcription factors like NEUROG1 and NEUROD1. However, this was accompanied by a relative downregulation of glial-associated transcription factors.

This transcription factor imbalance likely underlies the observed differentiation biases. In an immunocompetent environment, the interplay between pro-neuronal and pro-glial transcription factors is finely tuned by immune-derived signals. The absence of these signals in immunodeficient models disrupts this balance, potentially leading to suboptimal differentiation patterns that may not support full functional recovery.

Functional implications of altered NPC differentiation

The differentiation bias observed in our study—toward neurons in immunodeficient hosts and toward astrocytes in immunocompetent hosts—has significant functional implications. While neurons are essential for restoring neural circuits, astrocytes play crucial roles in supporting neuronal function, maintaining the blood-brain barrier, and modulating inflammation.[41]

The predominance of neuronal differentiation in immunodeficient hosts might seem advantageous at first glance. However, without the supportive functions of astrocytes and the myelinating capabilities of oligodendrocytes, these neurons may fail to integrate properly or function optimally. Conversely, the astrocytic bias seen in immunocompetent hosts might provide a more supportive environment for endogenous repair processes, even if it does not directly replace lost neurons.

Challenges in modeling the human immune response in rats

While our humanized RNU rat model offers valuable insights into the allogenic immune response to transplanted NPCs, it is essential to acknowledge its limitations. The model relies on the infusion of human PBMCs, which primarily consist of T and B cells, leaving other critical immune components, such as dendritic cells (DCs), natural killer (NK) cells, and macrophages, underrepresented.[42,43] These immune cells play pivotal roles in both innate and adaptive immunity and could significantly influence the outcome of NPC transplantation, particularly in terms of graft rejection or tolerance.[44]

Another potential limitation of the model is the risk of graft-versus-host disease (GVHD) due to the infused human PBMCs. GVHD, where donor immune cells attack the host's tissues, could affect NPC engraftment by exacerbating immune-mediated damage at the transplantation site.[45,46] Although GVHD is more commonly associated with stem cell or organ transplantation, the possibility of this occurring in the humanized rat model remains unclear and warrants further investigation. The absence or reduced complexity of these immune components in our model may limit its ability to fully replicate the intricate immune interactions that occur in humans. As a result, it is important to interpret our findings with caution, acknowledging that they may not capture the full spectrum of immune responses seen in clinical settings. To address these limitations, future studies should aim to incorporate a broader range of human immune cell populations to provide a more comprehensive understanding of the immune dynamics at play.

Limitations and future directions

While our study provides valuable insights into the impact of the immune environment on transplanted NPCs, it has several limitations. First, the use of rodent models, while necessary, may not fully recapitulate the human immune response to transplanted cells. Second, our study focused on a single time point post-transplantation; a longitudinal study could provide valuable insights into the temporal dynamics of NPC-immune cell interactions. Additionally, we used exclusively female rats to avoid potential complications like urinary tract infections in males, which could confound the results in SCI models. However, sex differences in immune responses and neuroinflammation are well-documented, with females often showing stronger immune reactions due to hormonal influences.[47] This could influence the outcomes of NPC transplantation, particularly under immunosuppressive conditions. Future studies should explore sex-specific responses to immunosuppression and cell transplantation to ensure broader clinical applicability.

While human PBMCs can simulate a human-like immune response, their persistence in a xenogeneic environment in rodents is indeed limited. Studies have demonstrated that human T cells can circulate in the peripheral blood of rats for a short period following injection. These cells typically remain detectable for up to 2-3 weeks, though their numbers gradually decline over time due to the onset of xenogeneic graft-versus-host disease (xGvHD), which restricts their longevity. Among the different cell populations, human T cells tend to persist longer than other immune cell types such as B cells or macrophages, which are more rapidly eliminated.[42-46,48-50] In future studies, a consistent supply of human PBMCs could be maintained through the use of methods such as human hematopoietic stem cell transplantation or prenatal humanization approaches.[50] While these methods offer valuable data, they also present considerable technical challenges and resource requirements. Nevertheless, despite these complexities, such models remain a powerful tool for better understanding the interactions between human immune cells and transplanted NPCs, particularly in a regenerative context like SCI. Future research could explore the feasibility of this approach in our context, as it would undoubtedly enhance the clinical relevance of NPC transplantation models.

Conclusion

Our findings highlight the critical role of immune cell-NPC interactions in determining the fate and functionality of transplanted cells in SCI. While immunodeficient models may enhance cell survival, they fail to recapitulate the complex signaling environment necessary for optimal NPC differentiation and integration. As the field moves towards clinical translation, these considerations will be crucial in

developing effective cell-based therapies for SCI that not only promote cell survival but also harness the beneficial aspects of the immune response to enhance functional recovery.

Acknowledgements

M.G.F. acknowledges support from the Robert Campeau Family Foundation/Dr. C.H. Tator Chair in Brain and Spinal Cord Research at UHN. N.H. acknowledges support from the Research Fund of the University of Basel for Excellent Junior Researchers. The authors would like to thank Dr. Tim Worden for editorial support.

Author contributions

Z.L., A.P., N.N., J.H., N.H., and J.C.T.C. contributed to data acquisition, experimental work, analysis and interpretation, and manuscript review and approval. M.K. and M.G.F. were responsible for study concept and design, data acquisition and analysis, and manuscript writing and approval. M.G.F. additionally secured funding, provided administrative support, and supplied study materials.

Funding

This study was supported by funding from Wings for Life, the Krembil Foundation, and Canadian Institutes of Health Research.

Conflict of interest

The authors declared no potential conflicts of interest.

Data availability

Data are available from the corresponding authors upon reasonable request.

Supplementary material

Supplementary material is available at *Stem Cells Translational Medicine* online.

References

1. Ahuja CS, Wilson JR, Nori S, et al. Traumatic spinal cord injury. *Nat Rev Dis Primers*. 2017;3:1-21.
2. Khazaei M, Ahuja CS, Fehlings MG. Induced pluripotent stem cells for traumatic spinal cord injury. *Front Cell Dev Biol*. 2016;4:152. https://doi.org/10.3389/fcell.2016.00152
3. Nagoshi N, Khazaei M, Ahlfors J-E, et al. Human spinal oligodendrogenic neural progenitor cells promote functional recovery after spinal cord injury by axonal remyelination and tissue sparing: oligodendrogenic NPCs for spinal cord injury. *Stem Cells Transl Med*. 2018;7:806-818. https://doi.org/10.1002/sctm.17-0269
4. Nakamura M, Okano H. Cell transplantation therapies for spinal cord injury focusing on induced pluripotent stem cells. *Cell Res*. 2013;23:70-80. https://doi.org/10.1038/cr.2012.171
5. Ahuja CS, Wilson JR, Nori S, et al. Traumatic spinal cord injury. *Nat Rev Dis Primers*. 2017;3:17018. https://doi.org/10.1038/nrdp.2017.18
6. Ahuja CS, Fehlings M. Concise review: bridging the gap: novel neuroregenerative and neuroprotective strategies in spinal cord injury. *Stem Cells Transl Med*. 2016;5:914-924. https://doi.org/10.5966/sctm.2015-0381
7. Popovich PG, Horner PJ, Mullin BB, Stokes BT. A quantitative spatial analysis of the blood–spinal cord barrier. *Exp Neurol*. 1996;142:258-275. https://doi.org/10.1006/exnr.1996.0196
8. David S, Kroner A, Greenhalgh AD, Zarruk JG, López-Vales R. Myeloid cell responses after spinal cord injury. *J Neuroimmunol*. 2018;321:97-108. https://doi.org/10.1016/j.jneuroim.2018.06.003
9. Allison DJ, Ditor DS. Immune dysfunction and chronic inflammation following spinal cord injury. *Spinal Cord*. 2015;53:14-18. https://doi.org/10.1038/sc.2014.184
10. Tran AP, Warren PM, Silver J. The biology of regeneration failure and success after spinal cord injury. *Physiol Rev*. 2018;98:881-917. https://doi.org/10.1152/physrev.00017.2017
11. Ankeny DP, Guan Z, Popovich PG. B cells produce pathogenic antibodies and impair recovery after spinal cord injury in mice. *J Clin Invest*. 2009;119:2990-2999. https://doi.org/10.1172/JCI39780
12. Mezey E, Chandross KJ, Harta G, Maki RA, McKercher SR. Turning blood into brain: cells bearing neuronal antigens generated in vivo from bone marrow. *Science*. 2000;290:1779-1782. https://doi.org/10.1126/science.290.5497.1779
13. Martino G, Pluchino S. The therapeutic potential of neural stem cells. *Nat Rev Neurosci*. 2006;7:395-406. https://doi.org/10.1038/nrn1908
14. Pluchino S, Zanotti L, Rossi B, et al. Neurosphere-derived multipotent precursors promote neuroprotection by an immunomodulatory mechanism. *Nature*. 2005;436:266-271. https://doi.org/10.1038/nature03889
15. Madsen JR, MacDonald P, Irwin N, et al. Tacrolimus (FK506) increases neuronal expression of GAP-43 and improves functional recovery after spinal cord injury in rats. *Exp Neurol*. 1998;154:673-683. https://doi.org/10.1006/exnr.1998.6974
16. Cao Q, Zhang YP, Howard RM, et al. Pluripotent stem cells engrafted into the normal or lesioned adult rat spinal cord are restricted to a glial lineage. *Exp Neurol*. 2001;167:48-58. https://doi.org/10.1006/exnr.2000.7536
17. Frisén J, Johansson CB, Török C, Risling M, Lendahl U. Rapid, widespread, and longlasting induction of nestin contributes to the generation of glial scar tissue after CNS injury. *J Cell Biol*. 1995;131:453-464. https://doi.org/10.1083/jcb.131.2.453
18. Sachewsky N, Hunt J, Cooke MJ, et al. Cyclosporin A enhances neural precursor cell survival in mice through a calcineurin-independent pathway. *Dis Models Mech*. 2014;7:953-961. https://doi.org/10.1242/dmm.014480
19. Hunt J, Cheng A, Hoyles A, Jervis E, Morshead CM. Cyclosporin A has direct effects on adult neural precursor cells. *J Neurosci* 2010;30:2888-2896. https://doi.org/10.1523/JNEUROSCI.5991-09.2010
20. Erlandsson A, Lin C-HA, Yu F, Morshead CM. Immunosuppression promotes endogenous neural stem and progenitor cell migration and tissue regeneration after ischemic injury. *Exp Neurol*. 2011;230:48-57.
21. Brooks CG, Webb PJ, Robins RA, et al. Studies on the immunobiology of rnu/rnu "nude" rats with congenital aplasia of the thymus. *Eur J Immunol*. 1980;10:58-65. https://doi.org/10.1002/eji.1830100112
22. Schwinzer R, Hedrich H-J, Wonigeit K. T cell differentiation in athymic nude rats (rnu/rnu): demonstration of a distorted t cell subset structure by flow cytometry analysis. *Eur J Immunol*. 1989;19:1841-1847. https://doi.org/10.1002/eji.1830191013
23. Hoornaert CJ, Le Blon D, Quarta A, et al. Concise review: innate and adaptive immune recognition of allogeneic and xenogeneic cell transplants in the central nervous system: CNS immune recognition of cellular grafts. *Stem Cells Transl Med.*. 2017;6:1434-1441. https://doi.org/10.1002/sctm.16-0434
24. Wu B, Matic D, Djogo N, et al. Improved regeneration after spinal cord injury in mice lacking functional T- and B-lymphocytes. *Exp Neurol*. 2012;237:274-285. https://doi.org/10.1016/j.expneurol.2012.07.016

25. Ziv Y, Ron N, Butovsky O, et al. Immune cells contribute to the maintenance of neurogenesis and spatial learning abilities in adulthood. *Nat Neurosci*. 2006;9:268-275. https://doi.org/10.1038/nn1629
26. Khazaei M, Ahuja CS, Rodgers CE, Chan P, Fehlings MG. Generation of definitive neural progenitor cells from human pluripotent stem cells for transplantation into spinal cord injury. In: Daadi MM, eds. *Neural Stem Cells*. Vol. 1919. Springer New York; 2019:25-41.
27. Khazaei M, Ahuja CS, Nakashima H, et al. GDNF rescues the fate of neural progenitor grafts by attenuating Notch signals in the injured spinal cord in rodents. *Sci Transl Med*. 2020;12:eaau3538. https://doi.org/10.1126/scitranslmed.aau3538
28. Russo J, Russo IH. *Techniques and Methodological Approaches in Breast Cancer Research*. Springer New York; 2014. https://doi.org/10.1007/978-1-4939-0718-2
29. Schneider T, Osl F, Friess T, Stockinger H, Scheuer WV. Quantification of human Alu sequences by real-time PCR--an improved method to measure therapeutic efficacy of anti-metastatic drugs in human xenotransplants. *Clin Exp Metastasis*. 2002;19:571-582. https://doi.org/10.1023/a:1020992411420
30. Veniaminova NA, Vassetzky NS, Kramerov DA. B1 SINEs in different rodent families. *Genomics*. 2007;89:678-686. https://doi.org/10.1016/j.ygeno.2007.02.007
31. Andersen J, Thom N, Shadrach JL, et al. Single-cell transcriptomic landscape of the developing human spinal cord. *Nat Neurosci*. 2023;26:902-914. https://doi.org/10.1038/s41593-023-01311-w
32. Hao Y, Stuart T, Kowalski MH, et al. Dictionary learning for integrative, multimodal and scalable single-cell analysis. *Nat Biotechnol*. 2024;42:293-304. https://doi.org/10.1038/s41587-023-01767-y
33. Durinck S, Spellman PT, Birney E, Huber W. Mapping identifiers for the integration of genomic datasets with the R/Bioconductor package biomaRt. *Nat Protoc*. 2009;4:1184-1191. https://doi.org/10.1038/nprot.2009.97
34. Chu T, Wang Z, Pe'er D, Danko CG. Cell type and gene expression deconvolution with BayesPrism enables Bayesian integrative analysis across bulk and single-cell RNA sequencing in oncology. *Nat Cancer* 2022;3:505-517. https://doi.org/10.1038/s43018-022-00356-3
35. Bierer BE, Holländer G, Fruman D, Burakoff SJ. Cyclosporin A and FK506: molecular mechanisms of immunosuppression and probes for transplantation biology. *Curr Opin Immunol*. 1993;5:763-773. https://doi.org/10.1016/0952-7915(93)90135-f
36. Neuhaus P, Blumhardt G, Bechstein WO, et al. Comparison of FK506- And cyclosporine-based immunosuppression in primary orthotopic liver transplantation: a single center experience. *Transplantation*. 1995;59:31-40. https://doi.org/10.1097/00007890-199501150-00007
37. Almawi WY, Melemedjian OK. Clinical and mechanistic differences between FK506 (tacrolimus) and cyclosporin A. *Nephrol Dialysis Transplant*. 2000;15:1916-1918. https://doi.org/10.1093/ndt/15.12.1916
38. van Gelder T, Hesselink DA. Mycophenolate revisited. *Transpl Int*. 2015;28:508-515. https://doi.org/10.1111/tri.12554
39. Nakanishi M, Niidome T, Matsuda S, et al. Microglia-derived interleukin-6 and leukaemia inhibitory factor promote astrocytic differentiation of neural stem/progenitor cells. *Eur J Neurosci*. 2007;25:649-658. https://doi.org/10.1111/j.1460-9568.2007.05309.x
40. Dombrowski Y, O'Hagan T, Dittmer M, et al. Regulatory T cells promote myelin regeneration in the central nervous system. *Nat Neurosci*. 2017;20:674-680. https://doi.org/10.1038/nn.4528
41. Sofroniew MV, Vinters HV. Astrocytes: biology and pathology. *Acta Neuropathol*. 2010;119:7-35. https://doi.org/10.1007/s00401-009-0619-8
42. Hesselton RM, Koup RA, Cromwell MA, et al. Human peripheral blood xenografts in the SCID mouse: characterization of immunologic reconstitution. *J Infect Dis*. 1993;168:630-640. https://doi.org/10.1093/infdis/168.3.630
43. Li Z, Yang X, Zhang Y, et al. A human peripheral blood mononuclear cell (PBMC) engrafted humanized xenograft model for translational Immuno-oncology (I-O) Research. *J Vis Exp*. 2019;150:59679. https://doi.org/10.3791/59679
44. Duchosal MA, Mauray S, Rüegg M, et al. Human peripheral blood leukocyte engraftment into SCID mice: critical role of CD4+ T cells. *Cell Immunol*. 2001;211:8-20. https://doi.org/10.1006/cimm.2001.1822
45. Lin AE, Reyes S, An X, et al. Experimental modeling of acute- and chronic-GvHD by xenotransplanting human donor PBMCs or cord blood CD34+ Cells (HSC) into NSG mice. *Blood*. 2018;132:5684-5684. https://doi.org/10.1182/blood-2018-99-115462
46. Janakiraman H, Becker SA, Bradshaw A, Rubinstein MP, Camp ER. Critical evaluation of an autologous peripheral blood mononuclear cell-based humanized cancer model. *PLoS One*. 2022;17:e0273076. https://doi.org/10.1371/journal.pone.0273076
47. Klein SL, Flanagan KL. Sex differences in immune responses. *Nat Rev Immunol*. 2016;16:626-638. https://doi.org/10.1038/nri.2016.90
48. Shiroki R, Poindexter NJ, Woodle ES, et al. Human peripheral blood lymphocyte reconstituted severe combined immunodeficient (hu-PBL-SCID) mice. A model for human islet allograft rejection. *Transplantation*. 1994;57:1555-1562.
49. Ladel CH, Püschner H, Kaufmann SH, Bamberger U. Human peripheral blood leukocytes transplanted on CB17 scid-scid mice are transferred to their offspring. *Eur J Immunol*. 1992;22:1735-1740. https://doi.org/10.1002/eji.1830220711
50. Mian SA, Anjos-Afonso F, Bonnet D. Advances in human immune system mouse models for studying human hematopoiesis and cancer immunotherapy. *Front Immunol*. 2021;11:619236. https://doi.org/10.3389/fimmu.2020.619236